TRAINING COURSE
ON

HYDROLOGICAL MODELING AND GIS

(MAY 26 TO JUNE 06, 2014)

FOR

UNFAO & Ministry of Energy and Water, Afghanistan

LECTURE NOTE
ON

HYDROLOGICAL MODELLING USING VIC

By

VAIBHAV GARG
IIRS DEHRADUN

NATIONAL INSTITUTE OF HYDROLOGY
AND
INDIAN ASSOCIATION OF HYDROLOGISTS

ROORKEE – 247 667 (UTTARAKHAND)

HYDROLOGICAL MODELING USING VARIABLE INFILTRATION CAPACITY MODEL

INTRODUCTION

Hydrological modeling is mathematical representation of natural processes which is generally defined largely by parameters and states, parameters being physical and generally time-variant descriptors of surface and subsurface characteristics, and states being fluxes and storages of water and energy that are propagated in time. Traditionally, hydrological models were developed to estimate or predict streamflow. Initially, a conceptual model namely Stanford Watershed Model (SWM) has been developed by Crawford and Linsley (1960), which represented the spatially lumped runoff response of the land surface to precipitation. Till today, the derivatives of SWM remain in use such as U.S. National Weather Service River Forecast System and Hydrologic Simulation Package Fortran. The applicability of such models is very limited as these models are useful for simulation of streamflow within the range of conditions for which they were developed. Also, the parameters of this type of models could not be related to physically measured quantities easily. Moreover, such models do not represent the effects of vegetation on evapotranspiration (ET) explicitly nor do they perform the surface energy balance[2].

In recent past, researchers have also developed models known as soil-vegetation-atmosphere transfer schemes (SVATS). These schemes have been explicitly developed to represent the land surface partitioning of net radiation into latent, sensible and ground heat fluxes in climate and weather forecast models. These models do consider the role of vegetation in estimation of ET, furthermore, these models do surface energy balance by iterating on one or more effective temperatures (Lettenmaier 2001). However, SVATS generally emphasis on vertical/column processes such as extraction of soil moisture by vegetation, and feedback between vegetation, soil moisture and surface atmospheric conditions that control transpiration. These models usually do not consider horizontal complexity/spatial heterogeneity of soil and vegetation, and topography which control runoff generation[3,4].

The Variable Infiltration Capacity (VIC) model has also been developed as a SVATS by Liang et al. (1994). VIC model is a semi-distributed macroscale hydrological model designed to represent surface energy, hydrological fluxes and states at scales from large river basins to the entire globe. Typically grid resolution ranges from 1/8 to 2 degree (http://www.hydro.washington.edu). VIC computes the vertical energy and moisture flux in grid cell based on specification at each grid cell considering soil properties and vegetation coverage. Also it includes the representation of sub grid variability in soil infiltration capacity and all mosaic of vegetation classes in any grid cell. It is a grid based semi distributed hydrological model which quantifies the dominant hydro-meteorological process taking place at the land surface atmospheric interface over large river basin to the entire globe. The distinguish features of VIC over other land surface models are as follows:

- it considers subgrid variability in land surface vegetation classes and explicitly represents its effects on water and energy budgets;
- the representation of soil moisture storage capacity as a spatial probability distribution at subgrid level, to estimate surface runoff (Zhao et al., 1980);
- its parameterization of drainage from the lower soil moisture zone (base flow) as a nonlinear recession (Dumenil and Todini, 1992);
- the model also incorporates the topography which in turn considers orographic precipitation and temperature lapse rate, hence, more realistic results for mountainous regions (Gao et al., 2009);
- the inclusion of both the saturation and infiltration excess runoff processes with a consideration of the subgrid-scale soil heterogeneity at model grid cell (Lohmann et al., 1998a,b; Liang and Xie, 2003);
- the frozen soil processes consideration for cold climate conditions (Cherkauer and Lettenmaier, 1999);
- it solves full surface energy and water balances (Gao et al., 2009);
- it has separate routing module based on a linear transfer function to simulate the streamflow;
- it also incorporates water management effects including reservoir operation, irrigation diversions and return flows (Haddeland et al., 2006a,b; Haddeland et al., 2007);
- it can be coupled with Global Circulation Models (GCM) and other climate models.

The resulted runoff is routed via a separate channel routing module to produce stream flow at selected point within the domain. Fig. 1 illustrates the Schema of the VIC model with a mosaic representation of vegetation coverage and three soil layers. VIC- 2L model was modified to VIC-3L by adding one thin surface layer along with a canopy layer to achieve better representation of bare soil evaporation processes after small summer rain fall event.

MAJOR COMPONENTS OF VIC MODEL

Vegetation cover

As shown in Fig. 2, VIC model surface is described by N+1 land cover types where n=1,...N represents N different vegetation and n=N+1 represents bare soil. All information related to vegetation is represented by vegetation library and vegetation parameter file. The land cover (vegetation) classes are specified by the fraction of the grid cell which they occupy, with their leaf area index (LAI), canopy resistance, surface albedo and relative fraction of roots in each of the soil layers.. According to the vegetation cover type within a grid cell infiltration, moisture flux between the soil layers and runoff are computed. Surface runoff and base flow are computed separately considering each vegetation type and then summed over the composition vegetation within each grid cell.

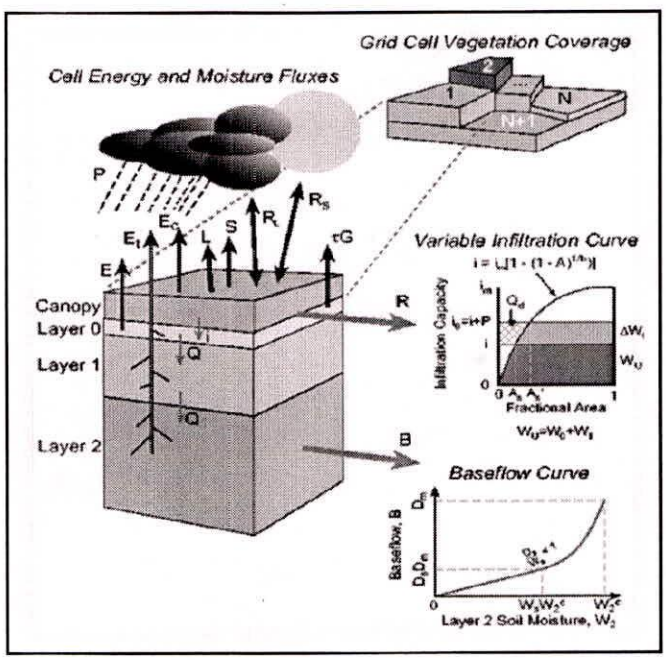

Fig. 1 Schema of Variable Infiltration Capacity Model

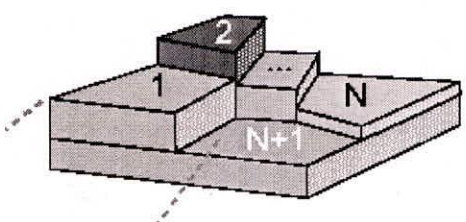

Fig. 2 Grid Cell Vegetation Coverage

Soil Layers

Soil characteristics can be represented for a user defined number of vertical layers usually two or three as seen in Fig. 1 dividing into thin upper layer and secondary set of layers. Soil parameters for each grid and soil layer is specified in user defined soil parameter file.

Rainfall

VIC model considers the sub-grid variability of precipitation which is distributed throughout all or a portion of grid cell as a function of rainfall intensity. Precipitation distribution can be expressed as follows,

$$\mu = (1\text{-}e^{-aI})$$

Where, I = Precipitation intensity, a = coefficient which describes the effect of grid cell size and geography.

Change in precipitation intensity of a storm changes the fractional coverage accordingly. When intensity increases, the fractional coverage over a grid cell increases and when decreased fractional coverage decreases. Before the occurrence of a storm the soil water content throughout the grid cell is set to average. However, forcing data plays an important role and accordingly simulation can be done hourly, 3 hourly, daily or monthly.

Snow Cover

VIC model is also capable of doing reliable simulation of snow pack process across a wide range of grid resolution in high altitude areas. Effect of vegetation cover on snow accumulation and melt is described internally within the VIC model through a coupled snow model.

WATER BALANCE MODE OF VIC MODEL

VIC model has capability to run in different modes viz. water balance, energy balance, frozen soil, etc. However, in the present study, water balance mode is used. Water balance mode assumes that land surface temperature equals air temperature. Although it does not solve the full surface energy balance, exception is the snow algorithm that still solves the surface energy balance to determine the fluxes needed to drive accumulation and ablation processes. It requires comparatively less time for computation than other modes due to removal of the ground heat flux solution and iterative procedure needed to close the surface energy balance. The time step ranges from hourly to daily.

The daily water balance mode is significantly faster than sub-daily simulations. Parameters required for daily solutions are different from those used for sub-daily solutions. Although the daily water balance model can be used to simulate discharge from a basin, calibration parameters for the daily water balance model are unlikely to be transferable to any model run with a sub-daily time step.

Evapotranspiration

The VIC model considers three types of evaporation: evaporation from the canopy layer (E_c, mm) of each vegetation tile, transpiration (E_t, mm) from each of the vegetation tiles, and evaporation from the bare soil (E_1, mm) (Liang et al. 1994). Total evapotranspiration over a grid cell is computed as the sum of the above components, weighted by the respective surface cover area fractions. The formulation of the total evapotranspiration is:

$$E = \sum_{n=1}^{N} C_n \cdot (E_{c,n} + E_{t,n}) + C_{N+1} \cdot E_1$$

Where C_n is the vegetation fractional coverage for the nth vegetation tile, C_{N+1} is the bare soil fraction, and $\sum_{n=1}^{N+1} C_n = 1$.

Canopy evaporation

When there is intercepted water on the canopy, the canopy evaporates at the maximum value. The maximum canopy evaporation (E_c^*, mm) from each vegetation tile is calculated using the following formulation:

$$E_c^* = \left(\frac{W_i}{W_{im}}\right)^{2/3} E_p \frac{r_w}{r_w + r_o}$$

Where W_{im} is the maximum amount of water the canopy can intercept (mm), which is 0.2 times LAI (Dickinson, 1984); the power of 2/3 is as described by Deardorff (1978). The architectural resistance, r_0, is caused by the variation of the humidity gradient between the canopy and the overlying air (s m^{-1}). In the model, r_0 is assigned for each land cover type according to the vegetation library. The aerodynamic resistance, r_w, represents the transfer of heat and water vapor from the evaporating surface into the air above the canopy (s m^{-1}). E_p is the potential evapotranspiration (mm) that is calculated from the Penman-Monteith equation (Shuttleworth, 1993) with the canopy resistance set to zero, which is:

$$\lambda_v E_p = \frac{\Delta(R_n - G) + \rho_a c_p (e_s - e_a)/r_a}{\Delta + \gamma}$$

where λ_v is the latent heat of vaporation (J kg^{-1}), R_n is the net radiation (W m^{-2}), G is the soil heat flux (W m^{-2}), $(e_s - e_a)$ represents the vapor pressure deficit of the air (Pa), ρ_a is the density of air at constant pressure (kg m^{-3}), c_p is the specific heat of the air (J kg^{-1} K^{-1}), Δ represents the slope of the saturation vapor pressure temperature relationship (Pa K^{-1}), and γ is the psychrometric constant (66 Pa K^{-1}). The Penman-Monteith equation as formulated above includes all parameters that govern the energy exchange and corresponding latent heat flux (evapotranspiration) from uniform expanses of vegetation.

The aerodynamic resistance (r_w, s m^{-1}) is described as follows after Monteith and Unsworth (1990):

$$r_w = \frac{1}{C_w u_z}$$

where u_z is the wind speed (m s^{-1}) at level z, and C_w is the transfer coefficient for water which is estimated taking into account the atmospheric stability. The algorithm for calculating C_w is based on Louis (1979).

When the continuous rainfall rate is lower than the canopy evaporation, the intercepted water is not sufficient for meeting the atmospheric demand within one time step. In such a case, the canopy evaporation (E_c, mm) is

$$E_c = f \cdot E_c^*$$

where f is the fraction of the time step for canopy evaporation to exhaust the intercepted water, and it is given by:

$$f = \min\left(1, \frac{W_i + P \cdot \Delta t}{E_c^* \cdot \Delta t}\right)$$

Vegetation transpiration

The vegetation transpiration (E^t, mm) is estimated using (Blondin, 1991; Ducoudre et al., 1993):

$$E_t = (1 - (\frac{W_i}{W_{im}})^{2/3}) E_p \frac{r_w}{r_w + r_o + r_c}$$

Where r_c is the canopy resistance (s m^{-1}) given by:

$$r_c = \frac{r_{0c} g_T g_{vpd} g_{PAR} g_{sm}}{LAI}$$

where r_{0c} is the minimum canopy resistance (s m^{-1}) according to the vegetation library, and g_T, g_{vpd}, g_{PAR}, and g_{sm} are the temperature factor, vapor pressure deficit factor, photosynthetically active radiation flux (PAR) factor, and soil moisture factor, respectively. Details about the four limiting factors are available through Wigmosta et al. (1994).

When canopy evaporation happens only for a fraction of the time step (f), the transpiration during that time step then has two parts as described by

$$E_t = (1-f)E_p \frac{r_w}{r_w + r_o + r_c} + f \cdot (1-(\frac{W_i}{W_{im}})^{2/3})E_p \frac{r_w}{r_w + r_o + r_c}$$

where the first term represents the part of the time step when there is transpiration but no canopy evaporation, and the second term represents the part of the time step when there is both evaporation from the canopy and transpiration.

The vegetation transpiration from a certain vegetation tile is the total contribution from all three soil layers, weighted by the fractions of roots in each layer.

Bare soil evaporation

The bare soil evaporation only occurs on the top thin layer. When the surface soil is saturated, it evaporates at the potential evaporation rate. When the top soil layer is not saturated, its evaporation rate (E_1) is calculated using the Arno formulation by Franchini and Pacciani (1991). The infiltration capacity (i) uses the spatially heterogeneous structure described by the Xianjiang Model (Zhao et al., 1980), which is expressed as

$$i = i_m(1-(1-A)^{1/b_i}) \quad \text{with} \quad i_m = (1+b_i)\cdot\theta_S \cdot |z|$$

where i_m is the maximum infiltration capacity (mm), A is the fraction of area for which the infiltration capacity is less than i, b_i is the infiltration shape parameter, θ_s is the soil porosity, and z is the soil depth (m). All these variables are for the top thin soil layer.

The bare soil evaporation is described as

$$E_1 = E_p\left(\int_0^{A_S} dA + \int_{A_S}^{1} \frac{i_0}{i_m(1-(1-A)^{1/b_i})} dA\right)$$

with A_s denoting the fraction of the bare soil that is saturated, and i_0 representing the corresponding point infiltration capacity.

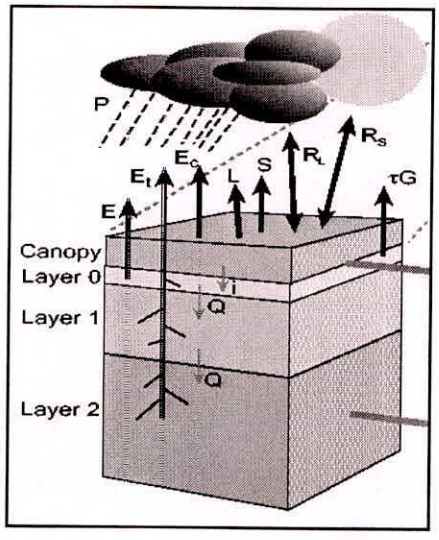

Fig 3: Cell Energy Components and Soil Layers

E - Evaporation from soil layer
E_t - Evapotranspiration
E_c- Canopy interception evaporation
L - Latent heat flux
S - Sensible heat flux
R_L - Long wave radiation,
R_S - Shortwave radiation
G - Ground heat flux
Q - Percolation

Bare soil evaporation

The bare soil evaporation only occurs on the top thin layer. When the surface soil is saturated, it evaporates at the potential evaporation rate. When the top soil layer is not saturated, its evaporation rate (E_l) is calculated using the Arno formulation by Franchini and Pacciani (1991). The infiltration capacity (i) uses the spatially heterogeneous structure described by the Xianjiang Model (Zhao et al., 1980), which is expressed as

$$i = i_m(1-(1-A)^{1/b_i}) \quad \text{with} \quad i_m = (1+b_i)\cdot\theta_S\cdot|z|$$

where i_m is the maximum infiltration capacity (mm), A is the fraction of area for which the infiltration capacity is less than i, b_i is the infiltration shape parameter, θ_s is the soil porosity, and z is the soil depth (m). All these variables are for the top thin soil layer.

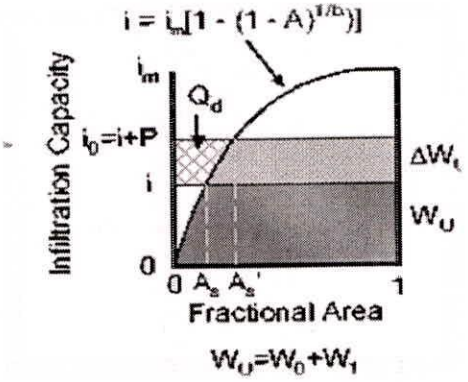

Fig 4 Infiltration Capacity Curve

The bare soil evaporation is described as

$$E_1 = E_p\left(\int_0^{A_s} dA + \int_{A_s}^{1} \frac{i_0}{i_m(1-(1-A)^{1/b_i})} dA\right)$$

with A_s denoting the fraction of the bare soil that is saturated, and i_0 representing the corresponding point infiltration capacity.

Soil Moisture and runoff

The VIC model uses the variable infiltration curve (Zhao et al., 1980) to account for the spatial heterogeneity of runoff generation. It assumes that surface runoff from the upper two soil layers is generated by those areas for which precipitation, when added to soil moisture storage at the end of the previous time step, exceeds the storage capacity of the soil. The formulation of subsurface runoff follows the Arno model conceptualization (Franchini and Pacciani, 1991; Todini, 1996). The soil moisture and runoff algorithms for the VIC-3L is explained with details in Liang et al. (1996).

Similar to the total evapotranspiration, the total runoff Q is expressed as:

$$Q = \sum_{n=1}^{N+1} C_n \cdot (Q_{d,n} + Q_{b,n})$$

where $Q_{d,n}$ (mm) and $Q_{b,n}$ (mm) are the direct runoff (surface runoff) and base flow (subsurface runoff) for the n^{th} land cover tile, respectively.

The VIC model assumes there is no lateral flow in the top two soil layers; therefore the movement of moisture can be characterized by the one-dimensional Richard's equation:

$$\frac{\partial \theta}{\partial t} = \frac{\partial}{\partial z}(D(\theta)\frac{\partial \theta}{\partial z}) + \frac{\partial K(\theta)}{\partial z}$$

where θ is the volumetric soil moisture content, $D(\theta)$ is the soil water diffusivity ($mm^2\ d^{-1}$), $K(\theta)$ is the hydraulic conductivity ($mm\ d^{-1}$), and z is soil depth (m). By including the atmospheric forcing, the integrated soil moisture for the top two soil layers can be described as (Mahrt and Pan, 1984):

$$\frac{\partial \theta_i}{\partial t} \cdot z_i = I - E - K(\theta)\Big|_{-z_1} + D(\theta)\frac{\partial \theta}{\partial z}\Big|_{-z_1} \qquad \text{(i=1,2)}$$

where I is the infiltration rate ($mm\ d^{-1}$), z_1 and z_2 are soil depth for layer 1 and layer 2, respectively. The infiltration rate I is the difference between the precipitation (or throughfall if there is vegetation coverage) and the direct runoff Q_d,

For the lower soil layer, an empirical formulation derived from large scale catchment hydrology is used in which the drainage and subsurface drainage are lumped together as base flow (Q_b). The soil moisture for the soil layer is described by the water balance equation including diffusion between soil layers as:

$$\frac{\partial \theta_3}{\partial t} \cdot (z_3 - z_2) = K(\theta)\Big|_{-z_2} + D(\theta)\frac{\partial \theta}{\partial z}\Big|_{-z_2} - E - Q_b$$

If it is bare soil, the evapotranspiration term E is zero because there is no evaporation from the lower soil layer. Otherwise, if the vegetation roots go through into the lower soil layer, the evapotranspiration term E needs to be considered.

Since the top thin soil layer has a very small water holding capacity, the direct runoff (surface runoff, Q_d) within each time step is calculated for the entire upper layer (layer 1 and layer 2) as (Liang et al., 1996):

$$Q_d = \begin{cases} P - z_2 \cdot (\theta_S - \theta_2) + z_2 \cdot \theta_S \cdot (1 - \dfrac{i_0 + P}{i_m})^{1+b_i}, & P + i_0 \le i_m \\ P - z_2 \cdot (\theta_S - \theta_2), & P + i_0 \ge i_m \end{cases}$$

where the infiltration capacity associated terms (i_0, i_m, θ_s, and b_i) are explained in bare soil evaporation.

The formulation of base flow (sub surface runoff, Q_b), which used the Arno model formulation, (Franchini and Pacciani, 1991), is expressed as:

$$Q_b = \begin{cases} \frac{D_S D_m}{W_S \theta_S} \cdot \theta_3, & 0 \le \theta_3 \le W_S \theta_S \\ \frac{D_S D_m}{W_S \theta_S} \cdot \theta_3 + (D_m - \frac{D_S D_m}{W_S})(\frac{\theta_3 - W_S \theta_S}{\theta_S - W_S \theta_S})^2, & \theta_3 \ge W_S \theta_S \end{cases}$$

where D_m is the maximum subsurface flow (mm d^{-1}), D_S is a fraction of D_m,, and W_S is the fraction of maximum soil moisture (soil porosity) θ_s. The base flow recession curve is linear below a threshold (W_S θ_s) and nonlinear above the threshold. The first derivative at the transition from the linear to nonlinear drainage is continuous.

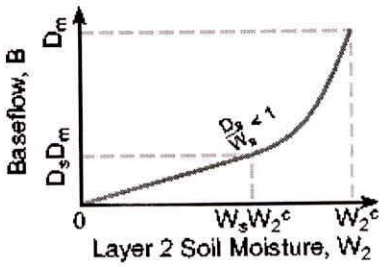

Fig 5 Baseflow Curve

THE ROUTING MODEL

The routing model is described in detail by Lohmann et al. (1996, 1998a). It essentially calculates the concentration time for runoff reaching the outlet of a grid cell as well as the channel flow in the river network. It is assumed that most horizontal flow within the grid cell reaches the channel network within the grid cell before it crosses the border into a neighboring grid cell. Flow can exit each grid cell in eight possible directions but all flow must exit in the same direction. The flow from each grid cell is weighted by the fraction of the grid cell that lies within the basin. Once water flows into the channel, it does not flow back out of the channel and therefore it is removed from the hydrological cycle of the grid cells. The daily surface runoff and baseflow produced by the VIC model from each grid cell is first transported to the outlet of the cell using a triangular unit hydrograph, and then routed to in the river network to the basin outlet.

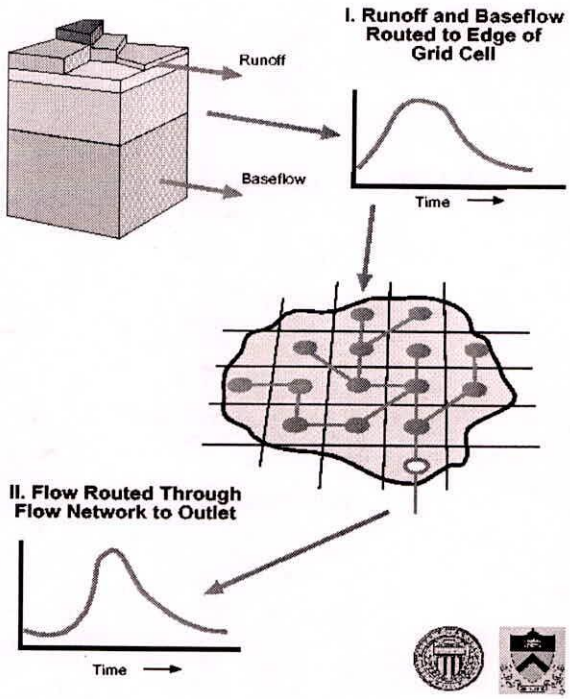

Fig. 6 Schematic of VIC network routing models

Both parts of the routing scheme (within grid cell and river routing) are constructed as simple linear transfer functions. The routing model extends the FDTF-ERUHDIT (First Differenced Transfer Function-Excess Rainfall and Unit Hydrograph by a Deconvolution Iterative Technique) approach (Duband et al., 1993) with a time scale separation and a simple linear river routing model. The model assumes that the runoff transport is linear, causal, stable, and time invariant. It also assumes the impulse response function is never negative. The following summarizes the within grid and river network routing respectively according to the modeling algorithms cited from Lohmann et al. (1996; 1998a).

Routing within a Grid Cell

To simulate the in-grid-dynamic of the horizontal routing process, one first separates the fast and slow components of the measured discharge with the linear model described in Duband et al., (1993):

$$\frac{dQ^S(t)}{dt} = -k \cdot Q^S(t) + b \cdot Q^F(t)$$

where $Q^S(t)$ is the slow flow, $Q^F(t)$ is the fast flow, and $Q(t)$ is the total flow with $Q(t) = Q^S(t) + Q^F(t)$.

For each river basin, the parameters b and k are assumed to be constant over the period of calculation. The ratio of b over k represents the ratio of water in the slow flow over water in the fast flow. The fast and slow components are analytically connected by:

$$Q^S(t) = b\int_0^t \exp(-k(t-\tau))Q^F(\tau)d\tau + Q^S(0)\exp(-kt)$$

The equation shows that the initial condition $Q^S(0)$ decays exponentially with the mean residence time of water in the flow ($1/k$) and the half-life decay is $T_{1/2}=(ln2)/k$. With discrete data the discharge equation can be solved with:

$$Q^S(t) = \frac{\exp(-k\cdot\Delta t)}{1+b\cdot\Delta t}Q^S(t-\Delta t) - \frac{b\cdot\Delta t}{1+b\cdot\Delta t}Q(t)$$

Based on the assumption that there is a linear relationship between measured streamflow and effective precipitation (P^{eff}, the part of the precipitation that becomes streamflow), it is sufficient to find an impulse response function connecting the fast component, Q^F, and P^{eff}, due to the analytical connection of the fast and slow components. This impulse response function and P^{eff} can be found by solving the following equation iteratively:

$$Q^F(t) = \int_0^{t_{max}} UH^F(\tau)P^{eff}(t-\tau)d\tau$$

In the equation $UH^F(\tau)$ is the impulse response function (also called unit hydrograph) for the fast flow component and t_{max} is the time taken for all fast processes to decay. The equation for Q^F can be expressed in its discrete format, in which there are n data points at the time step of Δt, and $t_{max} = (m-1)\cdot\Delta t$. Starting with the measured precipitation, the following discrete equation is solved iteratively for the calculation of UH_i^F.

$$\begin{pmatrix} Q_m^F \\ \vdots \\ Q_n^F \end{pmatrix} = \begin{pmatrix} P_m^{eff} & \cdots & P_1^{eff} \\ \vdots & \ddots & \vdots \\ P_n^{eff} & \cdots & P_{n-m+1}^{eff} \end{pmatrix} \begin{pmatrix} UH_0^F \\ \vdots \\ UH_{m-1}^F \end{pmatrix}$$

After each of the iteration steps the following constraint is applied:

$$\sum_{i=0}^{m-1} UH_i^F = \frac{1}{1+\frac{b}{k}} \text{ with } UH_i^F \geq 0 \;\forall i$$

The constraint results from the fixed fraction of the water in the fast and slow component, the fact that $\int_0^\infty UH(t)dt = 1$ and the non-negative assumption of UH(t). The calculated UH^F is then put into the following discrete equation to solve for P^{eff}.

$$\begin{pmatrix} Q_m^F \\ \vdots \\ \vdots \\ Q_n^F \end{pmatrix} = \begin{pmatrix} UH_{m-1}^F & \cdots & UH_0^F & 0 & \cdots & 0 \\ 0 & \ddots & \ddots & \ddots & \ddots & \vdots \\ \vdots & \ddots & \ddots & \ddots & \ddots & 0 \\ 0 & \cdots & 0 & UH_{m-1}^F & \cdots & UH_0^F \end{pmatrix} \begin{pmatrix} P_1^{eff} \\ \vdots \\ P_n^{eff} \end{pmatrix}$$

Again, after each iteration step the constraint ($0 \le P_i^{eff} \le Precipitation,\ \forall i$) is applied.

The newly calculated P^{eff} is then put back into the first discrete equation and the deconvolutions are repeated until convergence is reached. Grid cell impulse response functions can be obtained via deconvolution of the catchment impulse response function with the river network impulse response function belonging to that catchment (Lohmann *et al.*, 1996).

River Routing

The transport of water in channels is described using a simple linear river routing model, which follows the linearized Saint-Venant equation. The model assumes that water is transported out of the grid box only in the form of river flow. The following is the linearized Saint-Venant equation, where C and D are parameters denote wave velocity and diffusivity respectively.

$$\frac{\partial Q}{\partial t} = D\frac{\partial^2 Q}{\partial x^2} - C\frac{\partial Q}{\partial x}$$

Either from measurements or by estimation from geographical data of the river bed, C and D are regarded as effective parameters since there are often times more than one river in one grid cell. This way each grid cell ultimately ends up with one C and one D value, which characterize the water transport within the cell.

The Saint-Venant equation is solved with convolution integrals

$$Q(x,t) = \int_0^t U(t-s)h(x,s)ds$$

where

$$h(x,t) = \frac{x}{2t\sqrt{\pi D}} \exp(-\frac{(Ct-x)^2}{4Dt})$$

is the impulse response function of the Saint-Venant equation with h(x,0)=0 when x>0 and h(0,t)=δ(t) for t≥0. Because this solution scheme is linear and numerically stable, the influence from human activities (e.g., dams, irrigation water use) can be easily implemented in each node.

Further details of the VIC model can be found in Liang, 1994; Liang et. al, 1994; Liang et al. 1996; Lettenmaier, 2001. The VIC model runs in various modes namely energy balance, water balance and routing. VIC model has been validated and adopted at a range of spatial scales, from large river basins to continental and global scales. Within North America, it has been applied at 1° spatial resolution to the Missouri (Wood et al., 1997), Arkansas-Red river (Abdulla et al., 1996), Columbia river basins (Nijssen et al., 1997), and at 0.5° resolution to the Delaware River (Nijssen et al., 1997), Weser river basin in Germany (Lohmann et al., 1998a, b). The grid network version of the two layer VIC (VIC-2L) model together with a linear routing scheme was able to predict fairly accurately daily, monthly and annual streamflow. As a part of the Land Data Assimilation System project, Maurer et al. (2001a) carried out a detailed diagnosis of VIC model results of 50 years simulations over the central U.S. for model validation and parameterizations. Liang et al. (2004) adopted three layer VIC (VIC-3L) model to investigate the impacts of spatially distributed precipitation and soil heterogeneity on modeling water fluxes of blue river watershed (1,233 km^2 area), Oklahoma at different spatial resolutions. Yuan et. al. (2004) applied VIC-3L land surface model to simulate streamflow for the Hanjiang River basin in China. VIC-3L simulated daily runoff is routed to the outlets of six streamflow stations and compared with the daily and monthly observed streamflow at the stations. The results show that the model can simulate the observations well with reasonable accuracy.

References

Abdulla, F. A., Lettenmaier, D. P., Wood, E. F. and Smith, J. A., Application of a macroscale hydrologic model to estimate the water balance of the Arkansas-Red river basin. *J. Geophys. Res.*, 1996, **101(D3)**, 7449 - 7459.

Blondin, C. (1991), Parameterization of land-surface processes in numerical weather prediction, in *Land Surface Evaporation: Measurements and Parameterization*, edited by T. J. Schmugge and J. C. Andre, pp. 31-54, Springer-Verlag, New York.

Crawford, N. H. and Linsley, R. K., Computation of a synthetic streamflow record on a digital computer. *Int. Assoc. Sci. Hydrol. Publication*, 1960, **51**, 526 – 538.

Deardorff, J. W. (1978), Efficient prediction of ground surface-temperature and moisture, with inclusion of a layer of vegetation, *Journal of Geophysical Research-Oceans and Atmospheres*, *83*(NC4), 1889-1903.

Dickinson, R. E., A. Henderson-Sellers, P. J. Kennedy, M. F. Wilson (1986), Biosphere-atmosphertera nsfer scheme(BATS) for the NCAR community climate model, *NCAR Tech. Note TN-275 +STR.*

Duband, D., et al. (1993), Unit-hydrograph revised - an alternate iterative approach to UH and effective precipitation identification, *Journal of Hydrology*, *150*(1), 115-149.

Ducoudre, N. I., et al. (1993a), SECHIBA, a new set of parameterizations of the hydrologic exchanges at the land-atmosphere interface within the LMD atmospheric general circulation model, *J. Clim.*, *6*(2), 248-273.

Ducoudre, N. I., et al. (1993b), Sechiba, a New Set of Parameterizations of the Hydrologic Exchanges at the Land Atmosphere Interface within the Lmd Atmospheric General-Circulation Model, *J. Clim.*, *6*(2), 248-273.

Dumenil, L. and Todini, E., A rainfall-runoff scheme for use in the Hamburg climate model. In *Advances in Theoretical Hydrology, A Tribute to James Dooge*, (ed O'Kane, P.), 1992, European Geophysical Society Series on Hydrological Sciences **1**, pp. 129 - 157.

Franchini, M., and M. Pacciani (1991), Comparative-analysis of several conceptual rainfall runoff models, *Journal of Hydrology*, *122*(1-4), 161-219.

Gao, Z., Xhang, Z. and Zhang, X., Responses of water yield to changes in vegetation at a temporal scale. Front. *Forestry China*, 2009, **4(1)**, 53–59.

Haddeland, I., et al. (2006a), Effects of irrigation on the water and energy balances of the Colorado and Mekong river basins, Journal of Hydrology, 324(1-4), 210-223.

Haddeland, I., et al. (2006b), Anthropogenic impacts on continental surface water fluxes, Geophys Res Lett, 33(8), -.

Haddeland, I., et al. (2007), Hydrologic effects of land and water management in North America and Asia: 1700-1992, Hydrology and Earth System Sciences, 11(2), 1035-1045.

Lettenmaier, D. P., and F. Su (2009), in ARCTIC Climate Change-The ACSYS Decade and Beyond, edited, in press.

Lettenmaier, D. P., Present and future of modeling global environmental change: toward integrated modeling. In *Macroscale Hydrology: Challenges and Opportunities* (ed. Matsuno, T. and Kida, H.), 2001, pp. 111 - 136.

Liang, X., A two-layer variable infiltration capacity land surface representation for general circulation models. *Water Resour. Series* **TR140**, Univ. of Washington, Seattle, 1994.

Liang, X., and Z. H. Xie (2003), Important factors in land-atmosphere interactions: surface runoff generations and interactions between surface and groundwater, Global Planet Change, 38(1-2), 101-114.

Liang, X., et al. (1994), A SIMPLE HYDROLOGICALLY BASED MODEL OF LAND-SURFACE WATER AND ENERGY FLUXES FOR GENERAL-CIRCULATION MODELS, J. Geophys. Res.-Atmos., 99(D7), 14415-14428.

Liang, X., et al. (1996), Surface soil moisture parameterization of the VIC-2L model: Evaluation and modification, Global Planet Change, 13(1-4), 195-206.

Liang, X., et al. (1999), Modeling ground heat flux in land surface parameterization schemes, J. Geophys. Res.-Atmos., 104(D8), 9581-9600.

Liang, X., et al. (2003), A new parameterization for surface and groundwater interactions and its impact on water budgets with the variable infiltration capacity (VIC) land surface model, J. Geophys. Res.-Atmos., 108(D16).

Liang, X., et al. (2004), Assessment of the effects of spatial resolutions on daily water flux simulations, Journal of Hydrology, 298(1-4), 287-310.

Liang, X., Lattenmaier, D. P., Wood, E. F. and Burgess, S. J., A simple hydrologically based model of land surface, water, and energy flux for general circulation models. *J. Geophys. Res.*, 1994, **99(D7)**, 14,415-14,428.

Liang, X., Lettenmaier, D.P. and Wood, E.F., One-dimensional statistical dynamic representation of subgrid spatial variability of precipitation in the two-layer variable infiltration capacity model. *J. Geophys. Res.*, 1996, **101(D16)**, 21,403-21,422.

Lohmann, D., et al. (1996), A large scale horizontal routing model to be coupled to land surface parameterization schemes, Tellus(48A), 708-721.

Lohmann, D., et al. (1998a), Regional scale hydrology: I. Formulation of the VIC-2L model coupled to a routing model, Hydrol. Sci. J.-J. Sci. Hydrol., 43(1), 131-141.

Lohmann, D., et al. (1998b), Regional scale hydrology: II. Application of the VIC-2L model to the Weser River, Germany, Hydrol. Sci. J.-J. Sci. Hydrol., 43(1), 143-158.

Lohmann, D., et al. (2004), Streamflow and water balance intercomparisons of four land surface models in the North American Land Data Assimilation System project, J. Geophys. Res.-Atmos., 109(D7), 22.

Lohmann, D.E., Raschke, Nijssen, B. and Lettenmaier, D.P., Regional scale hydrology: I. Formulation of the VIC-2L model coupled to a routing model. *Hydrological Sciences Journal*, 1998a, **43(1)**, 131-141.

Lohmann, D.E., Raschke, Nijssen, B. and Lettenmaier, D.P., Regional scale hydrology:II. Application of the VIC-2L model to the Weser river, Germany. *Hydrological Sciences Journal*, 1998b, **43(1)**: 143-158.

Louis, J. F. (1979), Parametric Model of Vertical Eddy Fluxes in the Atmosphere, Bound-Lay Meteorol, 17(2), 187-202.

Mahrt, L., and H. Pan (1984), A 2-Layer Model of Soil Hydrology, Bound-Lay Meteorol, 29(1), 1-20.

Maurer, E. P., et al. (2001), Evaluation of the land surface water budget in NCEP/NCAR and NCEP/DOE reanalyses using an off-line hydrologic model, J. Geophys. Res.-Atmos., 106(D16), 17841-17862.

Maurer, E. P., et al. (2002), A long-term hydrologically based dataset of land surface fluxes and states for the conterminous United States, J. Clim., 15(22), 3237-3251.

Monteith, J. L., and M. H. Unsworth (1990), Principles of Environmental Physics, 2nd ed., Routledge, Chapman and Hall, New York.

Nijssen, B., et al. (1997), Streamflow simulation for continental-scale river basins, Water Resour Res, 33(4), 711-724.

Nijssen, B., et al. (2001a), Predicting the discharge of global rivers, J. Clim., 14(15), 3307-3323.

Nijssen, B., et al. (2001b), Global retrospective estimation of soil moisture using the variable infiltration capacity land surface model, 1980-93, J. Clim., 14(8), 1790-1808.

Nijssen, B., et al. (2003), Simulation of high latitude hydrological processes in the Torne-Kalix basin: PILPS phase 2(e) - 2: Comparison of model results with observations, Global Planet Change, 38(1-2), 31-53.

Wigmosta, M. S., et al. (1994), A DISTRIBUTED HYDROLOGY-VEGETATION MODEL FOR COMPLEX TERRAIN, Water Resour Res, 30(6), 1665-1679.

Wood, E. F., Global scale hydrology: advances in land surface modeling. *Reviews of Geophysics Supplement*, 1991, **29**, 193 -201.

Yuan, F., et al. (2004), An application of the VIC-3L land surface model and remote sensing data in simulating streamflow for the Hanjiang River basin, Canadian Journal of Remote Sensing, 30(5), 680-690.

Zhao, R.J., Zhang, Y.L., Fang, L.R., LIu, X.R. and Zhang, Q.S., The Xinanjiang model. In *Hydrological Forecasting Proceedings Oxford Symposium*, IASH, **129**, 1980, pp. 351 - 356.

****